ANALYSIS OF THE AIR-COOLING PROCESS OF BASIC SLAGS

Dirk Durinck, Peter Tom Jones, Bart Blanpain & Patrick Wollants
Katholieke Universiteit Leuven, Belgium

Sander Arnout
Innovatie- en Incubatie- Centrum, Belgium

ABSTRACT

About half of the slags generated worldwide in various pyrometallurgical processes are cooled to ambient temperatures using an air-cooling process at a slag yard. In this article, this air-cooling process is analysed on a microscopic level. The solidification mechanisms are determined using thermodynamic simulations and laboratory experiments. Industrial samples are used to validate the obtained results. Only basic slags are considered. Firstly a CaO-MgO-SiO_2 slag, which is independent of the oxygen partial pressure of the surrounding atmosphere, is investigated. Secondly the interaction with the surrounding atmosphere is also considered based on a CaO-CrO_x-SiO_2 slag. It is shown that during cooling (1) the interface between the liquid slag and the precipitating solid phases can be considered to be in thermodynamic equilibrium, (2) the diffusion in the solid phases is limited, (3) the diffusion in the liquid phase is rapid and (4) the oxygen exchange with the surrounding atmosphere is limited. In addition, the results also indicate that thermodynamic simulations can be used to accurately predict the end-mineralogy of air-cooled, basic slags.

INTRODUCTION

Slags are an indispensable tool for the pyrometallurgical industry to extract and purify metals. Large volumes are used annually, making slag one of the main by-products of the industry (Table 1). By far the largest slag producer is the iron and steelmaking industry with close to 400 million tons of slag in 2006. About two thirds of this slag originates from blast furnace processes, while the remaining third comes from steelmaking operations. Considerably less slag is formed during speciality steel and ferrous alloy production. However, the amount of stainless steel slag, for example, still added up to 9 million tons. The copper industry was responsible for approximately 30 million tons of slag, making it the main non-ferrous slag producer.

Table 1: Estimated slag production for the major pyrometallurgical industries in 2006 [1]

	Metal production $Mt_{/y}$	Slag/metal ratio t_{slag}/t_{metal}	Slag production Mt
Iron	872	0.25	218
Steel	1244	0.13	162
Stainless steel	28	0.3	9
Copper	15	2.2	33
Lead	8	2	16
Nickel	1.4	10	14
Phosphorus	1.1	8	9

Although these slags are by definition all oxidic in nature, their chemical composition varies significantly, as is shown in Figure 1. Iron, steel and phosphorus slags are calcium silicate slags, while copper and nickel slags are predominantly fayalite slags. Lead slag are situated in between.

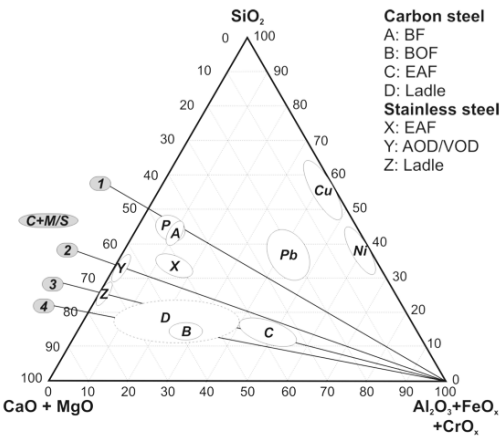

Figure 1: Slag compositions for the major pyrometallurgical industries (Adapted from [4])

After the metallurgical process, the high temperature slags are cooled to ambient temperatures to be further processed into a secondary resource or to be landfilled. The vast majority of slags are cooled either in a matter of seconds using a water granulation process or in matter of days using an air-cooling process at a slag yard. Alternative cooling processes are pelletisation, dry-granulation and slag expansion [5]. Now, as for metals, the cooling process can affect the microstructure and, therefore, the properties of the cooled slag greatly. Understanding the solidification mechanisms is instrumental to control and steer the cooling process to improve the quality of the end slag product.

Water granulated slags, mainly originating from iron and phosphorus production, are a high value resource for the cement industry, resulting in a utilisation level of nearly 100%. Air-cooled slags, on the other hand, are a low value resource that can be used as an aggregate in the construction industry. A significant fraction, however, is still internally stored or landfilled. Therefore, an investigation was started focussing on the air-cooling process. The goal was to understand how the high temperature slag composition can be linked to the mineralogy of the cooled slag product. The present work summarises the overall results obtained in this investigation. A more detailed discussion can be found in previous publications. [2, 3]

Macroscopic Analysis

Let us first examine the air-cooling process at a slag yard at a macroscopic level. The high temperature slag is poured from a slag pot onto a previous slag bed in consecutive layers of several centimetres (Figure 2). Due to the steep temperature gradient between the slag and the surrounding air atmosphere, heat is extracted from the slag. Because of the limited heat conductivity of slags, a temperature gradient inside the slag layer will develop. The edge of the slag layer cools rapidly, the centre slowly. The whole cooling process takes up to a day to reach temperatures below 100°C. This corresponds to an average cooling rate of about 1°C/min.

Besides the obvious temperature gradient between slag and atmosphere, also a gradient in oxygen partial pressure exists during cooling. The slag itself is in a reduced state due to the preceding contact with a metallic phase, while the surrounding air atmosphere is oxidising. As the oxygen partial pressure affects the oxidation state of transition elements such as Fe^{2+}/Fe^{3+} and Cr^{2+}/Cr^{3+}, this gradient can also affect the solidification behaviour of the slag.

Figure 2: The air-cooling process for metallurgical slags

METHODOLOGY

The problem is divided in two parts. In the first part, an oxygen partial pressure (pO_2) independent CaO-MgO-SiO_2 slag is investigated. In the second part, the interaction with the surrounding atmosphere is also considered based on a CaO-CrO_x-SiO_2 slag. The slag compositions are depicted below (Table 2). In both cases, thermodynamic simulations and laboratory experiments are used. The thermodynamic simulations allow for the calculation of the end mineralogy of the slags under various assumptions. Based on the

correspondence with the laboratory experiments, the actual solidification mechanisms are deduced. Industrial samples are used to validate the obtained results.

Table 2: Experimental slag compositions (in wt%)

	CaO	SiO_2	MgO	Cr_2O_3
pO_2 independent	48	37	15	/
pO_2 dependent	45	40	/	15

Thermodynamic Simulations

A slag solidification model was implemented using the ChemApp 5.1.6 programmers library for thermochemical applications. Thermodynamic data was gathered from the FactSage 5.4.1 database. Slags are equilibrated at 1640°C under a certain oxygen partial pressure. During cooling the following assumptions are imposed:

- Thermodynamic equilibrium at the solid/liquid interfaces in the slag
- Infinitely rapid diffusion in the liquid phase of the slag
- Infinitely *rapid* or *slow* diffusion in the solid phases of the slag
- *Open* or *closed* with respect to the surrounding atmosphere.

The detailed implementation is explained in previous publications. The simulations result in the slag mineralogy (in wt%) as a function of temperature. The mineralogy at ambient temperatures can be compared with experimental data.

Laboratory Experiments

For the laboratory experiments, starting slag powders were prepared from analytical grade $CaCO_3$, MgO, SiO_2 and Cr_2O_3 powders. After calcination of the $CaCO_3$, the powders were weighed; wet mixed in ethanol for 24 h using ZrO_2 milling balls and dried. Subsequently, about 20 g was put into a Pt-Rh crucible, which was loaded in a laboratory furnace. For the CaO-MgO-SiO_2 experiment, an open bottom loading furnace (AGNI - ELT 160-02 Springtype) was used. The CaO-CrO_x-SiO_2 experiment was performed in a closed GERO vertical tube furnace. The oxygen partial pressure in the furnace was controlled at around 10^{-10} atm using pre-defined flow rates of CO (500 ml/min), CO_2 (10 ml/min) and Ar (40 ml/min, < 2 ppm O_2). In both experiments, the slag was heated to 1640°C, equilibrated for 8 h and cooled at 1°C /min to ambient temperatures. The slag sample was removed from the crucible using a pneumatic scraping pen. It is important to notice that these experimental conditions do not fully match the industrial conditions, as in the lab experiments no sharp gradients in temperature or oxygen partial pressure along the gas/slag interface are present during solidification. Nevertheless, these experiments allow for a discussion on the industrial situation as well, as will be shown later in this article.

The phase composition of the experimental and industrial slag samples was determined by microstructural analysis. Slag specimens were embedded in a resin (Epofix) by vacuum impregnation, ground with diamond plates and polished with diamond paste. Carbon was evaporated on the sample surface to provide a conducting layer for microprobe analysis. Semi-quantitative (SQ) analyses were performed with a JEOL 733 electron probe microanalysis (EPMA) system equipped with an energy dispersive spectroscopy (EDS) system. Elemental distribution maps were measured with a Philips scanning electron microscope (SEM), also with an EDS system. The grid size and measuring time were set to 256 by 200 points and 1000 ms. Phase amounts were determined using quantitative X-ray powder

diffraction (XRD). Spectra were collected under ambient conditions with CuKα radiation (40kV and 40mA) in the range 20-70 °2θ using a Bragg-Brentano diffractometer. Counting time was 10 seconds for each 0.02 °2θ step. Quantitative results were obtained by refining the patterns adopting the Rietveld method.

RESULTS AND DISCUSSION

CaO-MgO-SiO_2

In Figure 3, the simulated solidification sequences for the CaO-MgO-SiO_2 slag are shown. The solid phases are indicated by their geological notation (C = CaO, S = SiO_2, M = MgO, K = Cr_2O_3). In both simulations thermodynamic equilibrium at the solid/liquid interface and rapid diffusion in the liquid phase are assumed. The diffusion in the solid phases is either infinitely rapid (left) or infinitely slow (right). As the CaO-MgO-SiO_2 slag is independent on oxygen partial pressure, no assumption on the interaction with the surrounding atmosphere is required.

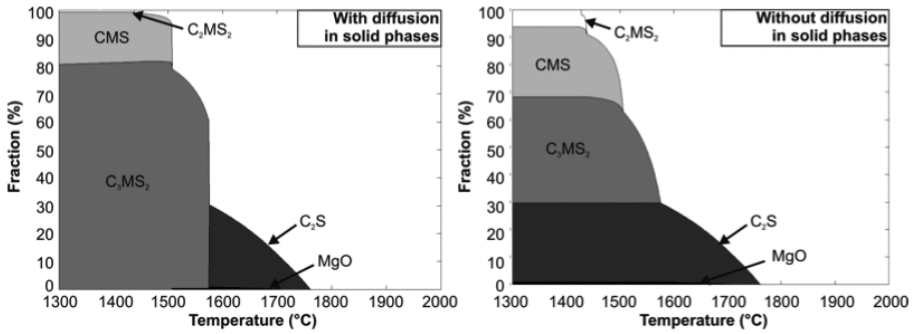

Figure 3: Simulated solidification sequences for the CaO-MgO-SiO_2 slag

The diffusion in the solid phases has a clear effect on both the solidification sequence and the end mineralogy. Initially, however, both simulations are identical. C_2S and MgO precipitate. Only at 1576°C, they diverge. Allowing diffusion in the solid phases, a peritectic reaction occurs:

$$L + C_2S + M \rightarrow C_3MS_2 \quad (1)$$

Such peritectic reaction can, however, not occur without diffusion in the solid phases. As a consequence, both simulations lead to different end levels in C_2S and MgO. As this kinetic barrier also affects the liquid phase composition, the solidification sequence below 1576°C also differs.

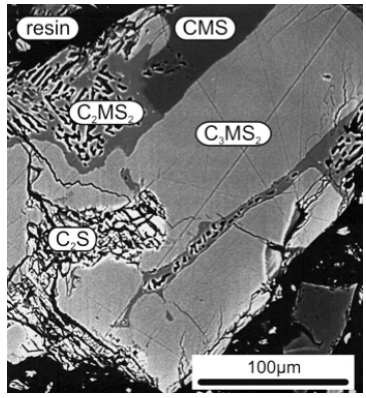

Figure 4: Back scattered electron (BSE) image of the experimental CaO-MgO-SiO_2 slag

In Figure 4, a BSE image of the fully solidified experimental CaO-MgO-SiO_2 slag is shown. The same phases as predicted by the simulations are encountered. MgO cannot be identified on the micrograph, but has been detected by XRD. The quantitative phase amounts determined by Rietveld refinement of the XRD pattern are compared to the simulated results in Figure 5. The experimental mineralogy corresponds best with the simulation assuming no diffusion in the solid phases. Qualitatively, this simulation predicts all phases accurately. Quantitatively, however, differences do exist, especially concerning the amount of C_2S. Nevertheless, despite these differences, this simulation predicts the experimental mineralogy far better than when diffusion in the solid phases is allowed. This demonstrates that during the solidification diffusion in the solid phases is in fact limited.

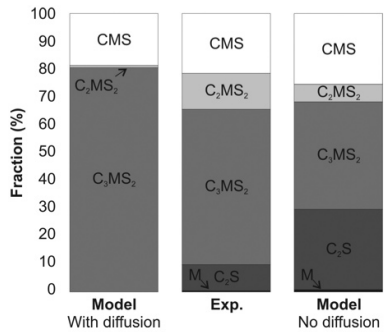

Figure 5: Experimental and simulated phase amounts in the CaO-MgO-SiO_2 slag

CaO-CrO_x-SiO_2

In Figure 6, the simulated solidification sequences for the CaO-CrO_x-SiO_2 slag are shown. Again, thermodynamic equilibrium at the solid/liquid interface and rapid diffusion in the liquid phase are assumed in both cases. Based on the previous results, the diffusion in the solid phases is not allowed. As the CaO-CrO_x-SiO_2 slag is dependent on oxygen partial pressure, an additional assumption on the interaction with the surrounding atmosphere is required. After initial equilibration of the slag in reducing conditions (pO_2 ~ 10^{-10} atm), the slag can be considered open to the surrounding atmosphere during cooling (left), allowing for oxygen transfer from the air to the slag. Alternatively, the slag can be considered closed off from the atmosphere (right).

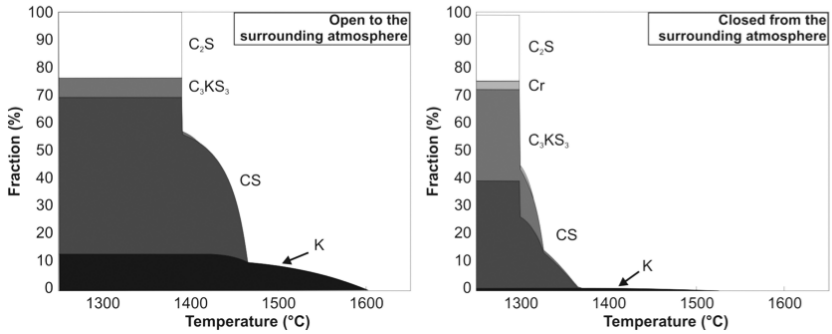

Figure 6: Simulated solidification sequences for the CaO-CrO_x-SiO_2 slag

The interaction with the surrounding atmosphere clearly affects the solidification sequence and the end mineralogy. The basic reason for this is the following. After equilibration in reducing conditions, the main fraction of the CrO_x in the slag is present as CrO. During cooling, it wants to oxidise to Cr_2O_3 according:

$$CrO + ½\ O_2 \rightarrow Cr_2O_3 \quad (2)$$

This reaction, however, requires oxygen transfer from the air to the slag. So, when the slag is considered closed from the atmosphere, it cannot take place. In this case, the CrO becomes thermodynamically unstable during further cooling, forming metallic chromium according to a disproportionation reaction:

$$3.CrO \rightarrow Cr^0 + Cr_2O_3 \quad (3)$$

In Figure 7, a BSE image of the fully solidified experimental CaO-CrO_x-SiO_2 slag is shown. Similar phases as predicted by the simulations are encountered. It is especially highlighted that small, metallic Cr particles are present throughout the slag microstructure, clearly indicating a lack of oxygen during solidification. The comparison between the experimental and simulated phase amounts, shown in Figure 8, points towards the same conclusion. Oxygen exchange with the surrounding atmosphere during solidification seems to be rather limited in the employed experimental setup.

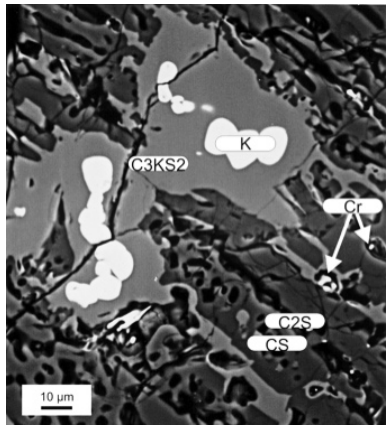

Figure 7: Back scattered electron (BSE) image of the experimental CaO-CrO_x-SiO_2 slag

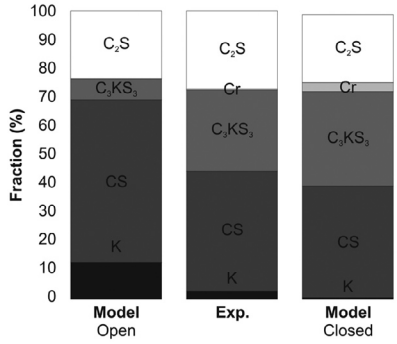

Figure 8: Experimental and simulated phase amounts in the $CaO\text{-}CrO_x\text{-}SiO_2$ slag

Industrial Validation

As the experimental conditions do not fully match the industrial conditions because of the lack of sharp gradients in temperature or oxygen partial pressure along the gas/slag interface, the obtained results need to be validated for industrial practice. In Figure 9, BSE images of two stainless steel slags are shown. In the AOD slag, a C_2S grain surrounded by C_3MS_2 is observed. As indicated above, if the diffusion in the solid phases would be sufficiently rapid, the C_2S would be consumed according to reaction (1). Therefore, its presence confirms the slow diffusion in the solid phases during solidification in industrial conditions.

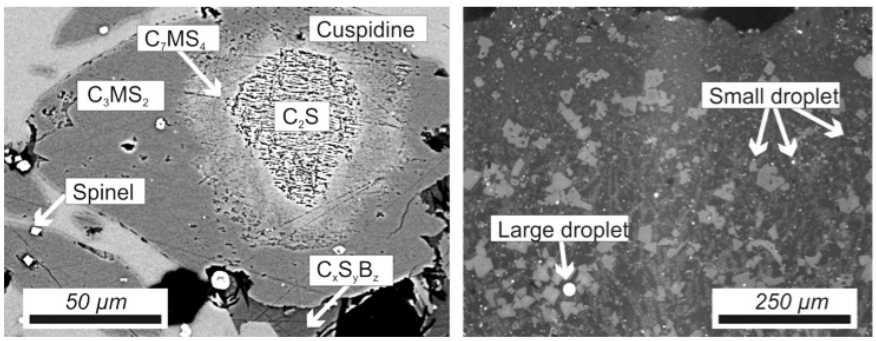

Figure 9: BSE image of two industrial stainless steel slags. (left: AOD slag; right EAF slag)

Besides a wide variety of oxidic minerals, two types of metal droplets are observed in the EAF slag. The large droplets (> 20 µm) have an austenitic stainless steel composition, containing iron, chromium and nickel. These droplets were entrapped from the metal bath in the slag during the metallurgical process. The majority of the smaller droplets (< 5 µm), on the other hand, contain also iron and chromium, but no nickel. The absence of nickel suggests that these droplets do not originate from the metal bath, but are formed inside the slag itself. It is believed that these particles are formed during cooling, confirming the $CaO\text{-}CrO_x\text{-}SiO_2$ experiment. One difference, however, is the combined presence of FeO and CrO in the slag. When the oxidisation to respectively Fe_2O_3 and Cr_2O_3 is obstructed by a lack of oxygen, first the following redox reaction occurs:

$$FeO + 2.CrO \rightarrow Fe^0 + Cr_2O_3 \quad (4)$$

FeO serves as an oxygen donor for CrO, as chromium is more reactive to oxygen. Only when FeO is depleted, the CrO disproportionates according reaction (3).

The observation of these Fe-Cr metal droplets suggests that also in industrial conditions only little oxygen is transferred from the surrounding air atmosphere to the slag during cooling. At first glance, this seems inconsistent with the nature of air-cooling. Indeed, at the slag yard, the reduced slag is in direct contact with air, which is a practically infinite source of oxygen. The authors' hypothesis to explain this paradox is that the steep temperature gradient between slag and air leads to the instantaneous formation of a solid layer at the top of the slag, which acts as a barrier for O^{2-} diffusion. Therefore, the bulk of the slag solidifies in a closed system.

This layer formation is corroborated by the sample of the industrial stainless steel EAF slag in Figure 9. The top of the image corresponds to the border of a slag layer. It can be seen that the bulk of the slag consist of a relatively coarse microstructure. At the edge itself, however, a fine microstructure is observed over a depth of approximately 250 μm, which indicates a higher cooling rate compared to the bulk of the slag. It must be remarked that this layer does contain large angular spinel particles, but these were already present at high temperature and did not form during cooling. It can also be seen that the edge of the slag does not contain any metallic droplets. The reason can be twofold. On the one hand, at the edge, the oxygen diffusion can be sufficient for the required oxidation reactions thereby, eliminating the need for the disproportionation reactions. On the other hand, the higher cooling rate can also inhibit the disproportionation reactions from occurring.

CONCLUSIONS

In this article, the air-cooling process of basic slags was analysed on a microscopic level. The solidification mechanisms were determined using thermodynamic simulations and laboratory experiments. It is shown that during air-cooling (1) the interface between the liquid slag and the precipitating solid phases can be considered to be in thermodynamic equilibrium, (2) the diffusion in the solid phases is limited, (3) the diffusion in the liquid phase is rapid and (4) the oxygen exchange with the surrounding atmosphere is limited. These conclusions are validated based on industrial stainless steel slag samples.

ACKNOWLEDGEMENTS

This work is performed with the financial and technical support of ArcelorMittal Stainless Genk and the IWT (project No. 050715).

REFERENCES

Durinck, D., Engström, F., Arnout, S., Heulens, J., Jones, T., Björkmann, B., Blanpain B. & Wollants, P. (2008a). *Review: Hot Stage Processing of Metallurgical Slags*. Resources, Conservation & Recycling, 52 (10), p. 1121-1131. [1]

Durinck, D., Mertens, G., Jones, P. T., Elsen, J., Blanpain, B. & Wollants, P. (2007). Slag Solidification Modelling using the Scheil-Gulliver Assumptions. *Journal of the American Ceramic Society*, 90 (4), pp. 1177–1185. [2]

Durinck, D., Jones, P. T., Blanpain, B. & Wollants, P. (2008b). Air-Cooling of Metallurgical Slags containing Multivalent Oxides. *Journal of the American Ceramic Society*, 91 (10) pp. 3342–3348. [3]

Motz, H. & Kuehn, M. (2004). *Iron and Steel Slags as Sustainable Construction Resources and Fertiliser*. Scanmet II - International Conference on Process Development in Iron and Steelmaking, Luleä, Sweden, June, p. 347-358. [4]

Mihok, L., Demeter, P., Baricova, D. & Seilerova, K. (2006). *Utilization of Ironmaking and Steelmaking Slags*. Metalurgija, 45 (3), pp. 163-168. [5]